OL Organic Letters

pubs.acs.org/OrgLett

Letter

Synthesis of *Adagrasib* (MRTX849), a Covalent KRAS^{G12C} Inhibitor Drug for the Treatment of Cancer

Cheng-yi Chen,* Zhichao Lu,* Thomas Scattolin, Chengsheng Chen, Yonghong Gan, and Mark McLaughlin

Cite This: *Org. Lett.* 2023, 25, 944–949

Read Online

ACCESS | Metrics & More | Article Recommendations | Supporting Information

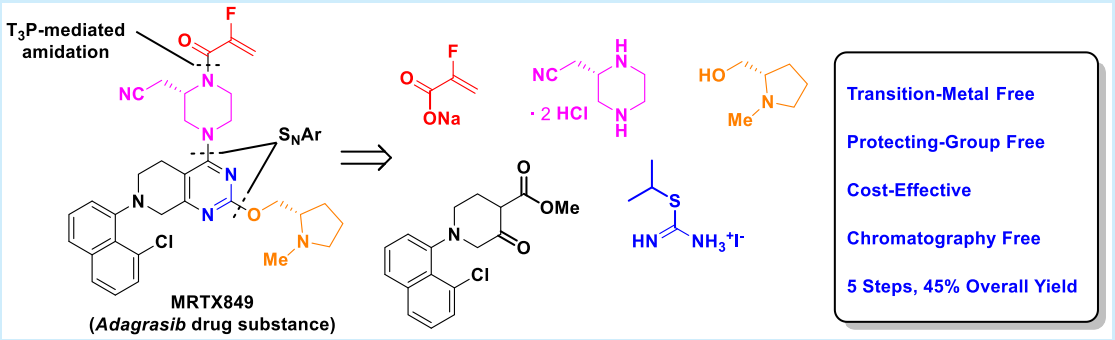

ABSTRACT: A concise, transition-metal and protection-free synthesis of *adagrasib* (MRTX849), a novel KRAS^{G12C} inhibitor drug recently approved by the FDA, is reported. Introduction of two chiral building blocks to the tetrahydropyridopyrimidine core was accomplished via two sequential S_NAr reactions. Extensive reaction optimization led to a robust, transition-metal-free oxidation of the sulfide intermediate. A judicious choice of the leaving group with favorable steric and electronic characteristics at the 4-OH position of the tetrahydropyridopyrimidine core enabled a facile S_NAr displacement to introduce the chiral piperazine. This new, five-step, chromatography-free synthesis of *adagrasib* from readily available starting materials obviated the palladium catalysis and protecting group manipulations in the current commercial route and significantly improved the efficiency of the process in 45% overall yield.

Kirsten rat sarcoma viral oncogene homologue (KRAS) is the notorious oncogene with the highest mutation rate among all cancers specifically associated with the top three most fatal cancers including pancreatic ductal adenocarcinoma (PDAC), non-small cell lung cancer (NSCLC), and colorectal cancer (CRC).[1] Furthermore, KRAS has been considered as a challenging therapeutic target, famously designated as "undruggable", and historically has had limited therapeutic options[1,2] until recent discovery of *sotorasib* (AMG510)[3] and *adagrasib* (MRTX849, **1** in Scheme 1)[4] as drugs targeting the G12C variant. *Adagrasib* (**1**) is a highly selective and potent covalent KRAS^{G12C} inhibitor, which has recently been approved as a monotherapy drug and is being evaluated in a combination therapy in patients with advanced KRAS^{G12C}-mutated solid tumors.[5−8] *Adagrasib* (**1**) was reported to show only mild side effects when combined with the immunotherapy drugs.[9] This positive clinical readout triggered the development of a more efficient process to this novel drug.

Adagrasib (MRTX849, **1**) features three distinct subunits: *N*-methyl prolinol, chloronaphthyl, and substituted piperazine attached to the tetrahydropyridopyrimidine core. A unique 2-fluoroacrylamide warhead located at the distal side of the piperazine is responsible for covalent binding to the target protein. As shown in Scheme 1, the current synthetic route started with a Boc-protected tetrahydropyridopyrimidine **2**.[10] A regioselective S_NAr reaction introduced the Cbz-masked piperazine moiety **3** at the more reactive 4-position. Installation of the prolinol subunit was achieved via palladium-catalyzed C−O bond formation between **4** at C-2 position and prolinol **5**. Introduction of the chloronaphthyl subunit required Boc-deprotection followed by a Buchwald-Hartwig amination of the resulting **6** with chloronaphthyl bromide **7**. Practical conditions employing 2-mercaptoethanol were developed to unmask the Cbz-protected piperazine to afford compound **9**.[11] *n*-Propanephosphonic acid anhydride (T_3P)-mediated coupling of **9** with the sodium 2-fluoroacrylate (**10**) completed the synthesis of *adagrasib* (**1**).

Received: December 20, 2022
Published: February 1, 2023

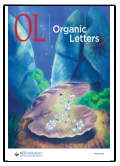

https://doi.org/10.1021/acs.orglett.2c04266
Org. Lett. 2023, 25, 944−949

Scheme 1. Current Manufacturing Process to *Adagrasib* (1)

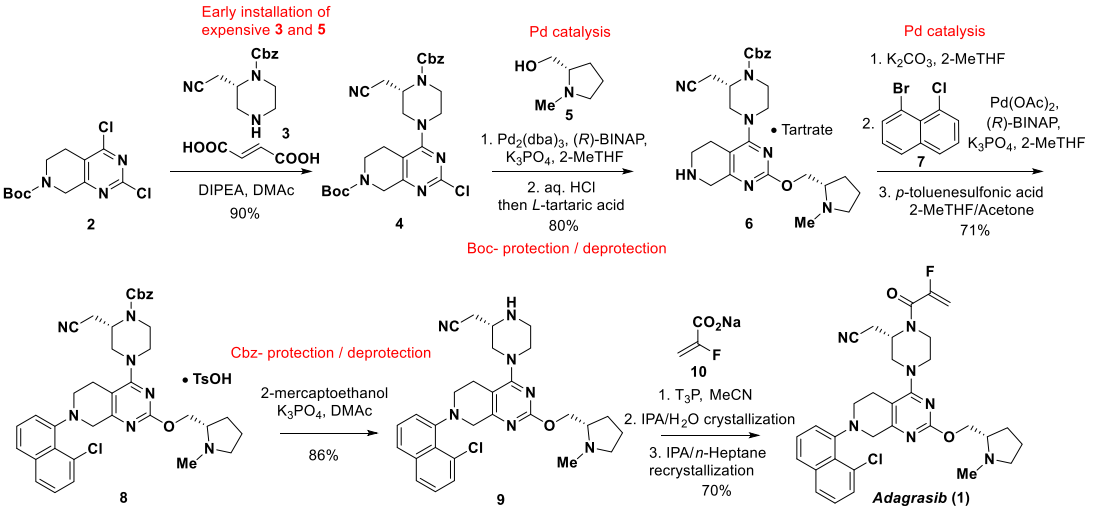

The current synthetic route has been employed to produce sufficient drug substance to support all the drug development activities including clinical studies and commercial launch. However, considering the overall efficiency, cost and sustainability, we identified three areas for further improvement (Scheme 1): (i) reducing or eliminating usage of expensive palladium catalysts/ligands in both C−O and C−N bond formations;[12] (ii) deferring the installation of the expensive chiral piperazine to a later stage in the synthesis; and (iii) avoiding protection/deprotection manipulations. Herein, we wish to report an efficient five-step synthesis of *adagrasib* (**1**) featuring late introduction of the costly piperazine and no need for the transition-metal catalysis or protecting groups.

The retrosynthesis of adagrasib featuring introduction of the costly chiral piperazine **12**[8] at a late stage of the synthesis is shown in Scheme 2. We intended to keep the last step in the new synthesis the same as the existing commercial launch route (Scheme 1). We conceived that penultimate **9** could be prepared from compound **11** and chiral piperazine **12** *via* a S_NAr reaction. Compound **11**, in turn, could be prepared from an appropriately activated pyrimidone (**13a** or **13b**) *via* another S_NAr reaction.[13,14] Ketoester **17** could be obtained using conventional chemistry and would serve as starting material for the construction of the tetrahydropyrido-pyrimidine core.[15]

The synthesis began with the preparation of ketoester **17** via a three-step through process. As shown in Scheme 3, the starting material **19** underwent two sequential alkylations: first with bromoester **20** to afford intermediate **21** and then with Weinreb amide **22** to afford intermediate **23**. Base-mediated intramolecular Dieckmann condensation of **23** afforded ketoester **17** in 60% overall yield. Notably, the use of Weinreb amide is essential to ensure the desired regioselectivity in the intramolecular Dieckmann condensation.[16]

With ketoester **17** in hand, a conventional two-step synthesis of sulfide **15a** via thiourea condensation/alkylation was initially assessed. As shown in Scheme 4, the condensation of ketoester **17** with thiourea afforded thiol **18** and the ensuing alkylation provided sulfide **15a** in good yield. However, this approach generated 2,4-bis-isopropylated side product **15c** which proved to be difficult to purge in the downstream process. In addition, sulfide **15a** contained residual iodide, which promoted severe

Scheme 2. Retrosynthesis of *Adagrasib* (1)

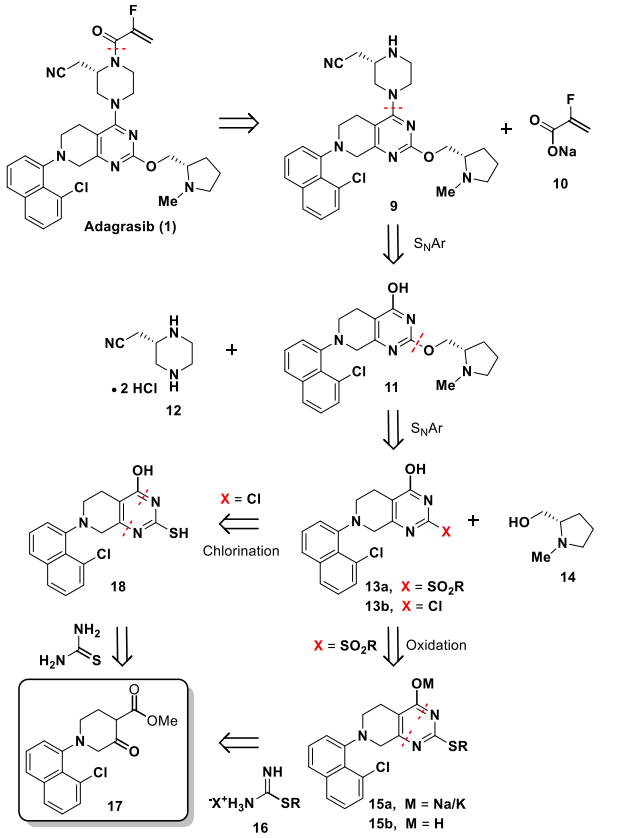

H_2O_2 degradation in the subsequent oxidation reaction, raising safety concerns for a scale-up.[17]

The formation of 2,4-bis-isopropylated side product **15c** was circumvented by forming **15a** via condensation of isopropyl isothiouronium iodide **16** with ketoester **17**. The discovery of intermediacy of amide **24** was consistent with a one-pot two-step sequence (Scheme 5). A more in-depth study of the physical properties of sulfide **15** unearthed that it could be crystallized in its neutral form **15b**. Indeed, simple acidic quench of the reaction afforded sulfide **15b** in 76% isolated yield and importantly without any detectable residual iodide.[18]

https://doi.org/10.1021/acs.orglett.2c04266
Org. Lett. 2023, 25, 944−949

Scheme 3. Synthesis of Ketoester 17

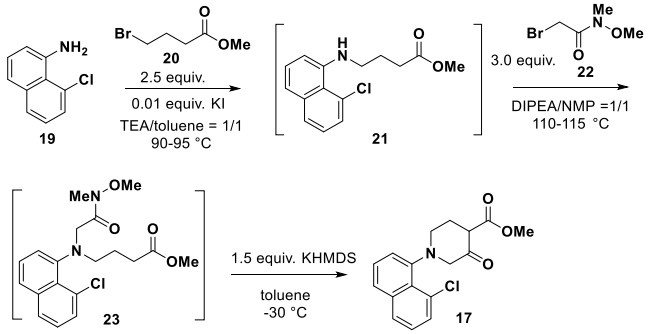

Scheme 4. Synthesis of Sulfone 13a from Ketoester 17

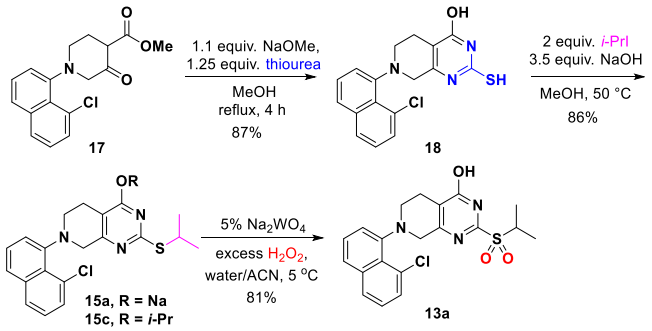

Scheme 5. New Route for Sulfone 13a and 11 Synthesis

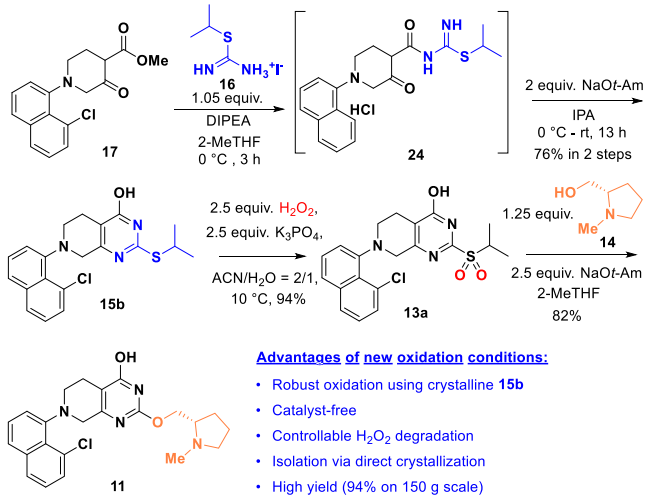

A search for favorable conditions to oxidize sulfide **15** to sulfone **13a** included exploration of a range of oxidants such as oxone, *m*-chloroperbenzoic acid and H_2O_2 with catalytic Na_2WO_4, all known to be viable for this type of transformation.[19−21] Employing H_2O_2 as the oxidant was particularly attractive due to its low cost, good atom economy and innocuous byproduct (water).[22] However, neutral sulfide **15b** (−OH form in Scheme 5) exhibited much poorer solubility than its salt **15a** (−ONa form) in most organic solvents. For this reason, *in situ* salt formation of sulfide **15a** for oxidation by pretreatment with NaOH was explored. Under these conditions, the sulfide was readily soluble in reasonable solvent volume and the oxidation of the *in situ* generated sodium salt **15a** proceeded quickly to afford sulfone product **13a** in 94% yield even in the absence of tungstate catalyst. However, significant H_2O_2 degradation in this strongly basic reaction medium (pH ≈ 14) posed safety concerns.[23,24]

It was reasoned that balancing sulfide solubility/reactivity versus H_2O_2 stability as a function of pH control could allow for efficient sulfide oxidation while minimizing unproductive H_2O_2 decomposition. Delightfully, we found that K_3PO_4 could resolve the issues described above (Scheme 5) as it readily converts the acidic pyrimidone sulfide **15b** to its soluble potassium salt and the resulting PO_4^{3-}/HPO_4^{2-} buffer solution maintains the reaction pH at ∼12, effectively suppressing the undesired H_2O_2 degradation. Optimal conditions for this tungstate-free oxidation were as follows: 2.5 equiv. H_2O_2 with 2.5 equiv. K_3PO_4 in acetonitrile−water mixtures at 10 °C.[25] At the end of reaction, acid quench of the reaction mixture enabled direct crystallization of the desired sulfone **13a** (94% yield on multihundred-gram scale). Sulfone **13a** sets the stage for prolinol installation via a S_NAr reaction (Scheme 5). Extensive screening of bases showed that 2.5 equiv of NaO*t*-Am gave the best yield, albeit with around 3% hydrolyzed side product which could be easily rejected in the downstream reactions.

An alternative route to intermediate **11** from compound **18** was also demonstrated (Scheme 6). Chlorination of **18** with

Scheme 6. Alternative Synthesis of Intermediate 11

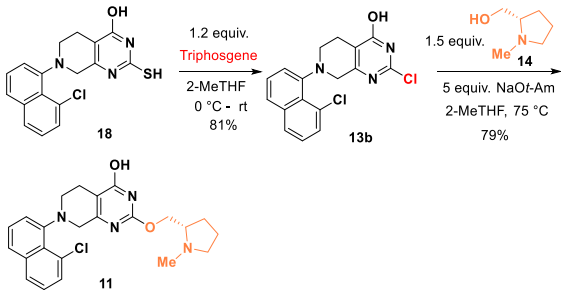

triphosgene selectively converted 2-SH group to 2-Cl with the 4-OH remaining intact and provided **13b** in 81% yield.[26] The chloropyrimidine performs equally well in the S_NAr reaction using prolinol **14** to give compound **11** in 79% yield. This approach with better atom economy is complementary to the sulfone route (Scheme 5).

For the installation of the piperazine unit, the conversion of **11** to **9** could be accomplished in a two-step through process sequence as shown in Scheme 7. For example, activation of the OH group in **11** via either Tf_2O or $PhNTf_2$, followed by S_NAr displacement afforded intermediate **9** in 70% and 78% yield, respectively (Scheme 7A, for details: see the SI). Preliminary screening of different leaving groups such as −OMs or −OTs showed significant amount of apparent hydrolysis to regenerate starting material (**11**) (Scheme 7B).

Based on these observations, we continued to explore alternatives to the −OTf leaving group to determine if the yield and purity profile could be improved and to better understand the mechanistic pathways involved in this S_NAr process. Focusing on tosylate **25b**, we initially speculated side-product **11** might come from hydrolysis of the intermediate **25**. However, reaction in the presence of activated molecular sieves still gave the same reaction profile. The labeling experiment by adding $H_2{}^{18}O$ to the reaction solution did not form any ^{18}O-labeled side product. In contrast, a tosylated piperazine **26** was identified as the sole byproduct. These results indicated that

https://doi.org/10.1021/acs.orglett.2c04266
Org. Lett. 2023, 25, 944−949

Scheme 7. S_NAr Reaction Using Piperazine 12

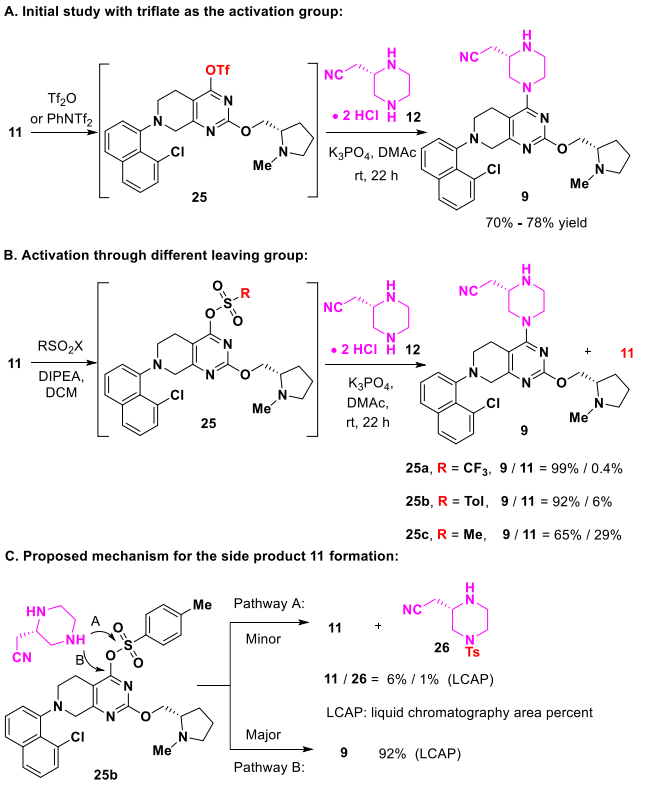

side product **11** did not result from the hydrolysis of intermediate **25**. Rather, it was generated through a nucleophilic attack of the free piperazine nitrogen at the sulfur of the sulfonate (Pathway A in Scheme 7C). The major pathway with the attack at the carbon center of the pyrimidine ring affords the desired product **9** (Pathway B in Scheme 7C).

The formation of the side product **26** suggested that *ortho*-substituents on the benzene ring of the sulfonates might inhibit the Pathway A due to the steric effect of the *ortho* group, and consequently suppress the formation of **11** (Pathway B). To explore this hypothesis, we screened various substituted benzenesulfonates as the leaving groups for this S_NAr reaction. As shown in Figure 1, 2-NO_2, 2-Cl, 2,4-di-Cl, 2,6-di-Cl substituted benzenesulfonates with strong electron-withdrawing and steric effects exhibited a desirable reaction profile with much less side product **11** formed. When the readily available 2-nitrobenzenesulfonate was used (Scheme 8), the telescoped activation-S_NAr process afforded product **9** in 90% yield and excellent purity.[27] Finally, *n*-propanephosphonic acid anhydride (T_3P)-mediated amidation of **9** with **10** afforded *adagrasib* (**1**) in 85% yield.[10,28] It should be noted that using sodium acrylate **10** instead of the free acid minimized the decomposition of the acid and obviated the use of amine base in the T_3P mediated coupling.

In summary, a new, transition-metal and protection-free synthesis of *adagrasib* (MRTX849, **1**) has been developed. This chromatography-free synthesis proceeds in five linear steps to produce *adagrasib* (MRTX849, **1**) in 45% overall yield and with excellent quality. This approach takes advantage of a late-stage installation of the costly chiral subunits onto the tetrahydropyridopyrimidine core by two sequential S_NAr reactions. The new synthesis obviates palladium catalysis and protecting group manipulations, which were necessary in the existing commercial route. A robust, catalyst-free oxidation of

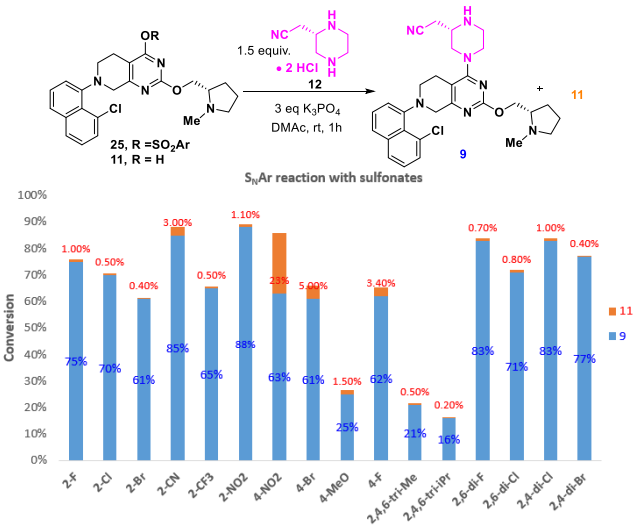

Figure 1. Sulfonate screening for 2nd S_NAr reaction.

Scheme 8. 2nd S_NAr Reaction and Amidation

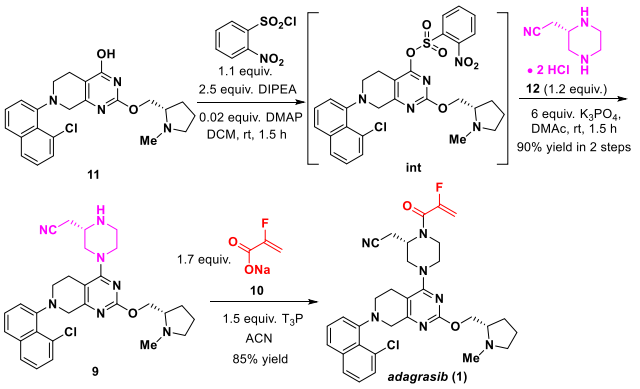

sulfide also alleviated safety concerns caused by the H_2O_2 degradation. The study on the leaving groups shows both steric and electronic effect enhanced the efficiency of the S_NAr reaction. We believe this newly developed route offers a preferred means to produce the important anticancer therapeutic *adagrasib* (**1**). Furthermore, the methodology developed here could be applied to modular syntheses of analogues of the $KRAS^{G12C}$ inhibitors.[29]

■ ASSOCIATED CONTENT

Data Availability Statement

The data underlying this study are available in the published article and its Supporting Information.

Supporting Information

The Supporting Information is available free of charge at https://pubs.acs.org/doi/10.1021/acs.orglett.2c04266.

Experimental details, NMR data, and characterization for all new compounds (PDF)

■ AUTHOR INFORMATION

Corresponding Authors

Cheng-yi Chen − *Chemical Process R&D, Mirati Therapeutics, San Diego, California 92121, United States;* orcid.org/0000-0001-7666-3087; Email: chenc@mirati.com

https://doi.org/10.1021/acs.orglett.2c04266
Org. Lett. 2023, 25, 944−949

Zhichao Lu − *Chemical Process R&D, Mirati Therapeutics, San Diego, California 92121, United States*; Email: luz@mirati.com

Authors

Thomas Scattolin − *Chemical Process R&D, Mirati Therapeutics, San Diego, California 92121, United States*; orcid.org/0000-0002-2950-2456

Chengsheng Chen − *Chemical Process R&D, Mirati Therapeutics, San Diego, California 92121, United States*

Yonghong Gan − *Chemical Process R&D, Mirati Therapeutics, San Diego, California 92121, United States*

Mark McLaughlin − *Chemical Process R&D, Mirati Therapeutics, San Diego, California 92121, United States*

Complete contact information is available at: https://pubs.acs.org/10.1021/acs.orglett.2c04266

Notes

The authors declare no competing financial interest.

■ ACKNOWLEDGMENTS

The authors are grateful to WuXi STA, PharmaBlock China and US for the general support in chemistry; to Stanley Yu (Mirati Therapeutics) and Todd Baumgartner (Mirati Therapeutics) for the analytical support; and to Dr. Michał Achmatowicz (Mirati Therapeutics) for the helpful discussion during the preparation of the manuscript.

■ REFERENCES

(1) Huang, L.; Guo, Z.; Wang, F.; Fu, L. KRAS Mutation: from Undruggable to Druggable in Cancer. *Signal Transduct. Target. Ther.* **2021**, *6*, 386−405.

(2) Désage, A.-L.; Léonce, C.; Swalduz, A.; Ortiz-Cuaran, S. Targeting KRAS Mutant in Non-Small Cell Lung Cancer: Novel Insights Into Therapeutic Strategies. *Front. Oncol.* **2022**, *12*, 1−19.

(3) Zhang, L.; Griffin, D. J.; Beaver, M. G.; Blue, L. E.; Borths, C. J.; Brown, D. B.; Caille, S.; Chen, Y.; Cherney, A. H.; Cochran, B. M.; Colyer, J. T.; Corbett, M. T.; Correll, T. L.; Crockett, R. D.; Dai, X.-J.; Dornan, P. K.; Farrell, R. P.; Hedley, S. J.; Hsieh, H.-W.; Huang, L.; Huggins, S.; Liu, M.; Lovette, M. A.; Quasdorf, K.; Powazinik, W. I. V.; Reifman, J.; Robinson, J. A.; Sangodkar, R. P.; Sharma, S.; Kumar, S. S.; Smith, A. G.; St-Pierre, G.; Tedrow, J. S.; Thiel, O. R.; Truong, J. V.; Walker, S. D.; Wei, C. S.; Wilsily, A.; Xie, Y.; Yang, N.; Parsons, A. T. Development of a Commercial Manufacturing Process for Sotorasib, a First-in-Class $KRAS^{G12C}$ Inhibitor. *Org. Process Res. Dev.* **2022**, *26*, 3115−3125.

(4) Adagrasib is marketed under the brand name Krazati, see: https://www.krazati.com.

(5) Jänne, P. A.; Riely, G. J.; Gadgeel, S. M.; Heist, R. S.; Ou, S.-H. I.; Pacheco, J. M.; Johnson, M. L.; Sabari, J. K.; Leventakos, K.; Yau, E.; Bazhenova, L.; Negrao, M. V.; Pennell, N. A.; Zhang, J.; Anderes, K.; Der-Torossian, H.; Kheoh, T.; Velastegui, K.; Yan, X.; Christensen, J. G.; Chao, R. C.; Spira, A. I. Adagrasib in Non-Small-Cell Lung Cancer Harboring a $KRAS^{G12C}$ Mutation. *N. Engl. J. Med.* **2022**, *387*, 120−131.

(6) Ou, S.-H. I.; Jänne, P. A.; Leal, T. A.; Rybkin, I. I.; Sabari, J. K.; Barve, M. A.; Bazhenova, L.; Johnson, M. L.; Velastegui, K. L.; Cilliers, C.; Christensen, J. G.; Yan, X.; Chao, R. C.; Papadopoulos, K. P. First-in-Human Phase I/IB Dose-Finding Study of Adagrasib (MRTX849) in Patients With Advanced $KRAS^{G12C}$ Solid Tumors (KRYSTAL-1). *J. Clin. Oncol.* **2022**, *40*, 2530−2538.

(7) Hallin, J.; Engstrom, L. D.; Hargis, L.; Calinisan, A.; Aranda, R.; Briere, D. M.; Sudhakar, N.; Bowcut, V.; Baer, B. R.; Ballard, J. A.; Burkard, M. R.; Fell, J. B.; Fischer, J. P.; Vigers, G. P.; Xue, Y.; Gatto, S.; Fernandez-Banet, J.; Pavlicek, A.; Velastagui, K.; Chao, R. C.; Barton, J.; Pierobon, M.; Baldelli, E.; Patricoin, E. F., III; Cassidy, D. P.; Marx, M. A.; Rybkin, I. I.; Johnson, M. L.; Ou, S.-H. I.; Lito, P.; Papadopoulos, K. P.; Jänne, P. A.; Olson, P.; Christensen, J. G. The $KRAS^{G12C}$ Inhibitor MRTX849 Provides Insight toward Therapeutic Susceptibility of KRAS-Mutant Cancers in Mouse Models and Patients. *Cancer Discovery* **2020**, *10*, 54−71.

(8) Fell, J. B.; Fischer, J. P.; Baer, B. R.; Blake, J. F.; Bouhana, K.; Briere, D. M.; Brown, K. D.; Burgess, L. E.; Burns, A. C.; Burkard, M. R.; Chiang, H.; Chicarelli, M. J.; Cook, A. W.; Gaudino, J. J.; Hallin, J.; Hanson, L.; Hartley, D. P.; Hicken, E. J.; Hingorani, G. P.; Hinklin, R. J.; Mejia, M. J.; Olson, P.; Otten, J. N.; Rhodes, S. P.; Rodriguez, M. E.; Savechenkov, P.; Smith, D. J.; Sudhakar, N.; Sullivan, F. X.; Tang, T. P.; Vigers, G. P.; Wollenberg, L.; Christensen, J. G.; Marx, M. A. Identification of the Clinical Development Candidate MRTX849, a Covalent $KRAS^{G12C}$ Inhibitor for the Treatment of Cancer. *J. Med. Chem.* **2020**, *63*, 6679−6693.

(9) Ledford, H. Cancer drugs are closing in on some of the deadliest mutations. *Nature* **2022**, *610*, 620−622.

(10) Snead, D.; Gan, Y.; Scattolin, T.; Paymode, D.; Achmatowicz, M.; Rudisill, D., et al. Development of Adagrasib's Commercial Manufacturing Route. *ChemRxiv.*; Cambridge Open Engage: Cambridge, 2022. DOI: 10.26434/chemrxiv-2022-9b3s1.

(11) Scattolin, T.; Gharbaoui, T.; Chen, C.-y. A Nucleophilic Deprotection of Carbamate Mediated by 2-Mercaptoethanol. *Org. Lett.* **2022**, *24*, 3736−3740.

(12) Palladium price has risen dramatically (≈ $100,000/kg) over the past decade and remains highly volatile: Williams, G. *Palladium Price Update: H1 2022, Investing news Network*, 2022. https://investingnews.com/daily/resource-investing/precious-metals-investing/palladium-investing/palladium-price-update/.

(13) Hoffmann-Emery, F.; Niedermann, K.; Rege, P. D.; Konrath, M.; Lautz, C.; Kraft, A. K.; Steiner, C.; Bliss, F.; Hell, A.; Fischer, R.; Carrera, D. E.; Beaudry, D.; Angelaud, R.; Malhotra, S.; Gosselin, F. Development of a Practical and Greener Process for the Dual Leucine Zipper Kinase Inhibitor GDC-0134 Comprising Two SNAr Reactions, Oxidation and Suzuki Coupling. *Org. Process Res. Dev.* **2022**, *26*, 313−322.

(14) Li, C.; Haeffner, F.; Wang, S.; Yuan, C.; Shang, D.; Shi, X.; Ma, B.; Hopkins, B. T.; O'Brien, E. M. Sulfone Displacement Approach for Large-Scale Synthesis of 4-Chloro-N-(1-methyl-1H-pyrazol-4-yl) pyrimidin-2-amine. *Org. Process Res. Dev.* **2022**, *26*, 137−143.

(15) Brown, T. H.; Blakemore, R. C.; Durant, G. J.; Emmett, J. C.; Ganellin, C. R.; Parsons, M. E.; Rawlings, D. A.; Walker, T. F. Isocytosine H2-receptor Histamine Antagonists I. Oxmetidine and Related Compounds. *Eur. J. Med. Chem.* **1988**, *23*, 53−62.

(16) Intramolecular Dieckmann condensation of bis-ester was explored and the reaction is not regioselective.

(17) Hansen, J. C. The Iodide-Catalyzed Decomposition of Hydrogen Peroxide: A Simple Computer-Interfaced Kinetics Experiment for General Chemistry. *J. Chem. Educ.* **1996**, *73*, 728−732.

(18) Upon screening of various alkyl groups in the condensation reaction, the *i*-Pr thiourea showed superior reaction performance and highest isolated yield. For experimental details, see the SI.

(19) Liu, N.-W.; Liang, S.; Manolikakes, G. Recent Advances in the Synthesis of Sulfones. *Synthesis* **2016**, *48*, 1939−1973.

(20) Matavos-Aramyan, S.; Soukhakian, S.; Jazebizadeh, M. H. Selected Methods for the Synthesis of Sulfoxides and Sulfones with Emphasis on Oxidative Protocols. *Phosphorus, Sulfur Silicon Relat. Elem.* **2020**, *195*, 181−193.

(21) (a) Laudadio, G.; Straathof, N. J. W.; Lanting, M. D.; Knoops, B.; Hessel, V.; Noël, T. An Environmentally Benign and Selective Electrochemical Oxidation of Sulfides and Thiols in a Continuous-flow Microreactor. *Green Chem.* **2017**, *19*, 4061−4066 Electrochemical oxidation was also reported recently:. (b) Bottecchia, C.; Lehnherr, D.; Lévesque, F.; Reibarkh, M.; Ji, Y.; Rodrigues, V. L.; Wang, H.; Lam, Y.-h.; Vickery, T. P.; Armstrong, B. M.; Mattern, K. A.; Stone, K.; Wismer, M. K.; Singh, A. N.; Regalado, E. L.; Maloney, K. M.; Strotman, N. A. Kilo-Scale Electrochemical Oxidation of a

Thioether to a Sulfone: A Workflow for Scaling up Electrosynthesis. *Org. Process Res. Dev.* **2022**, *26*, 2423−2437.
(22) Shilcrat, S. Process Safety Evaluation of a Tungsten-Catalyzed Hydrogen Peroxide Epoxidation Resulting In a Runaway Laboratory Reaction. *Org. Process Res. Dev.* **2011**, *15*, 1464−1469.
(23) Galbács, Z. M.; Csányi, L. J. Alkali-induced Decomposition of Hydrogen Peroxide. *J. Chem. Soc., Dalton Trans.* **1983**, 2353−2357.
(24) Koubek, E.; Haggett, M. L.; Battaglia, C. J.; Ibne-Rasa, K. M.; Pyun, H. Y.; Edwards, J. O. Kinetics and Mechanism of the Spontaneous Decompositions of Some Peroxoacids, Hydrogen Peroxide and *t*-Butyl Hydroperoxide. *J. Am. Chem. Soc.* **1963**, *85*, 2263−2268.
(25) Jereb, M. Highly Atom-Economic, Catalyst- and Solvent-Free Oxidation of Sulfides into Sulfones Using 30% Aqueous H_2O_2. *Green Chem.* **2012**, *14*, 3047−3052 Under these conditions, sulfone was formed through sulfoxide intermediate. For an example of catalyst-free oxidation of sulfide with H_2O_2, see:.
(26) Callingham, M.; Blum, F.; Pavé, G. One-Step Synthesis of 2-Chloropyrimidin-4-ol Derivatives: An Unusual Reactivity of Thiophosgene. *Org. Lett.* **2015**, *17*, 4930−4932.
(27) The S_NAr reaction of **12** is regioselective as shown in reference 8.
(28) The current process with no impurity > 0.08% detected is under evaluation for commercialization of the drug.
(29) We are actively exploring this area and will report it in due course.

https://doi.org/10.1021/acs.orglett.2c04266
Org. Lett. 2023, 25, 944−949